Origins and impacts of dynamical diquark correlations

Jorge Segovia

U. Pablo de Olavide, en Sevilla

UNIVERSIDAD PABLO DE OLAVIDE SEVILLA

The 10th International Conference on Quarks and Nuclear Physics (QNP 2024)

Facultat de Biologia, Universitat de Barcelona

July 8-12, 2024

Quantum Chromodynamics in its non-perturbative regime

Emergence

Low-level rules producing high-level phenomena with enormous apparent complexity

Start from the QCD Lagrangian:

$$\mathcal{L}_{\rm QCD} = \bar{\psi}(i\not{D} - m)\psi - \frac{1}{4} G_a^{\mu\nu} G_{\mu\nu}^a + \frac{1}{2\xi}(\partial^\mu A_\mu^a)^2 + \partial^\mu \bar{c}^a \partial_\mu c^a + g\, f^{abc}(\partial^\mu \bar{c}^a) A_\mu^b c^c \,.$$

Lattice-regularized QCD, Continuum Schwinger-function methods, ...

And obtain:

- Dynamical generation of fundamental mass scale in pure Yang-Mills (gluon mass).
- Quark constituent masses and dynamical chiral symmetry breaking.
- Bound state formation: mesons, baryons, glueballs, hybrids, multiquark systems...
- Signals of confinement.

These (emergent) phenomena is not apparent in the QCD Lagrangian; however, they characterized the nonperturbative regime of QCD where hadrons live

Emergent phenomena *could be associated with dramatic, dynamically driven changes in the analytic structure of QCD's Schwinger functions, which are solutions of the DSEs*

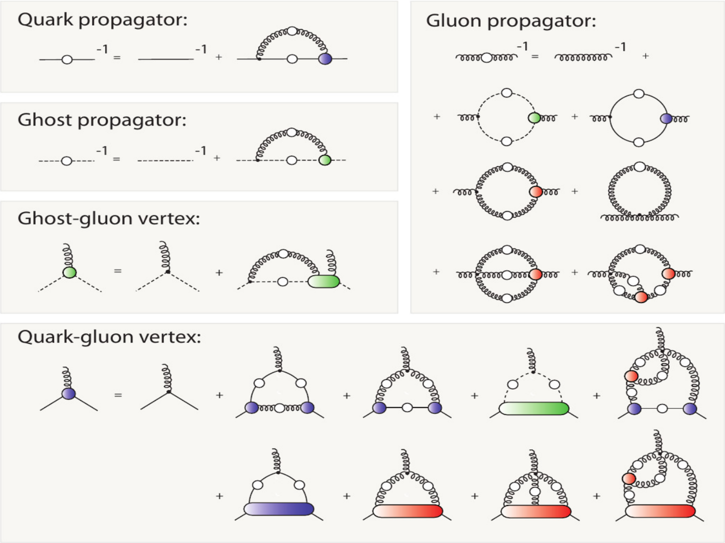

☞ Dressed-gluon propagator in Landau gauge:

$$i\Delta_{\mu\nu} = -iP_{\mu\nu}\mathbf{\Delta(q^2)}, \quad P_{\mu\nu} = g_{\mu\nu} - q_\mu q_\nu/q^2$$

- An inflexion point at $q^2 > 0$.
- Breaks the axiom of reflexion positivity.
- Gluon mass generation $\leftrightarrow$ Schwinger mechanism.

A.C. Aguilar *et al.*, Phys. Rev. D78 (2008) 025010;
I.L. Bogolubsky *et al.*, Phys. Lett. B676 (2009) 69.

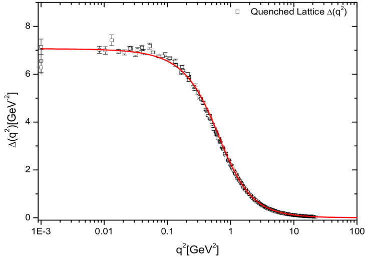

☞ Dressed-ghost propagator in Landau gauge:

$$G^{ab}(q^2) = \delta^{ab}\frac{\mathbf{J(q^2)}}{q^2}$$

- No power-like singular behavior at $q^2 \to 0$.
- Good indication that $J(q^2)$ reaches a plateau.
- Saturation of ghost's dressing function.

Ph. Boucaud *et al.*, JHEP 0806 (2008) 099;
C. Fischer *et al.*, Annals Phys. 324 (2009) 2408.

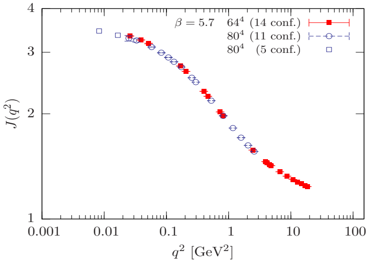

D. Binosi *et al.*, Phys. Rev. D96 (2017) 054026;
A. Deur *et al.*, Prog. Part. Nucl. Phys. 90 (2016) 1-74.

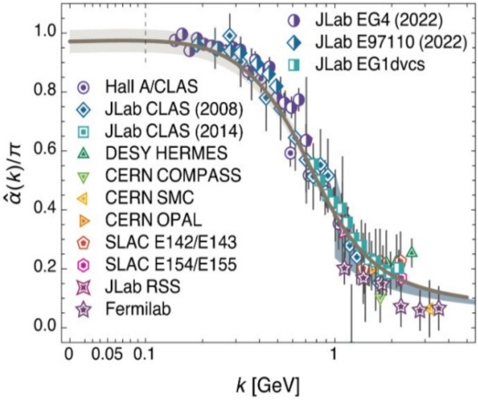

- Data = running coupling defined from the Bjorken sum-rule.

$$\int_0^1 dx \left[g_1^p(x,k^2) - g_1^n(x,k^2) \right] = \frac{g_A}{6}\left[1 - \frac{1}{\pi}\alpha_{g_1}(k^2)\right]$$

- Curve determined from combined continuum and lattice analysis of QCD's gauge sector (massless ghost and massive gluon).
- The curve is a running coupling that does NOT depend on the choice of observable.
  - No parameters.
  - No matching condition.
  - No extrapolation.
- It predicts and unifies an enormous body of empirical data via the matter-sector bound-state equations.

- Perturbative regime:

$$\alpha_{g_1}(k^2) = \alpha_{\overline{\rm MS}}(k^2)\left[1 + 1.14\alpha_{\overline{\rm MS}}(k^2) + \ldots\right]$$

$$\hat{\alpha}_{\rm PI}(k^2) = \alpha_{\overline{\rm MS}}(k^2)\left[1 + 1.09\alpha_{\overline{\rm MS}}(k^2) + \ldots\right]$$

Non-perturbative QCD: Dynamical generation of quark mass

☞ Dressed-quark propagator in Landau gauge:

$$S^{-1}(p) = Z_2(i\gamma\cdot p + m) + \Sigma(p) = \left(\frac{Z(p^2)}{i\gamma\cdot p + \mathbf{M(p^2)}}\right)^{-1}$$

- Mass generated from the interaction of quarks with the gluon-medium.
- Light quarks acquire a HUGE constituent mass.
- Responsible of the 98% of proton's mass, the large splitting between parity partners, ...

M.S. Bhagwat *et al.*, Phys.Rev. C68 (2003) 015203.

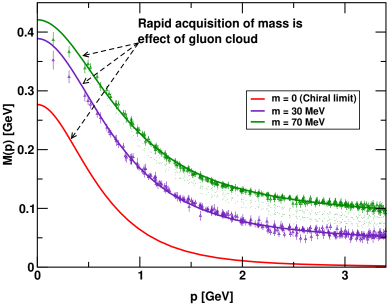

☞ Goldberger-Treiman relation at the quark level:

Quark propagator: $S^{-1}(p) = i\gamma\cdot p\, A(p^2) + B(p^2)\,,$

Pion's BS-amplitude: $\Gamma_\pi(p,P) \propto \gamma^5 E_\pi(p;P)\,.$

$$\mathbf{f_\pi E_\pi(p;0) = B(p^2)}$$

Properties of the massless pion are a direct measure of the dressed-quark mass function

Cleanest expression of the mechanism that is responsible for almost all the visible mass in the universe

Diquark correlations

Any interaction able to create Goldstone modes as bound-states of light dressed-quark and -antiquark will generate strong $\bar{3}_c$ correlations between any two dressed quarks.

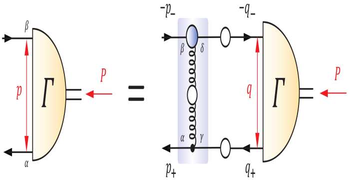

Meson BSE

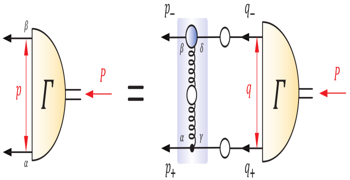

Diquark BSE

☞ Owing to properties of charge-conjugation, a diquark with spin-parity J^P may be viewed as a partner to the analogous J^{-P} meson:

$$\Gamma_{q\bar{q}}(p;P) = -\int \frac{d^4q}{(2\pi)^4}\, g^2 D_{\mu\nu}(p-q)\frac{\lambda^a}{2}\gamma_\mu\, S(q+P)\Gamma_{q\bar{q}}(q;P)S(q)\,\frac{\lambda^a}{2}\,\gamma_\nu$$

$$\Gamma_{qq}(p;P)C^\dagger = -\frac{1}{2}\int \frac{d^4q}{(2\pi)^4}\, g^2 D_{\mu\nu}(p-q)\frac{\lambda^a}{2}\gamma_\mu\, S(q+P)\Gamma_{qq}(q;P)C^\dagger S(q)\,\frac{\lambda^a}{2}\,\gamma_\nu$$

☞ Whilst no pole-mass exists, the following mass-scales express the strength and range of the correlation:

$$m_{[ud]_{0^+}} = 0.7-0.8\,\text{GeV}, \quad m_{\{uu\}_{1^+}} = 0.9-1.1\,\text{GeV}, \quad m_{\{dd\}_{1^+}} = m_{\{ud\}_{1^+}} = m_{\{uu\}_{1^+}}$$

☞ Diquark correlations are soft, they possess an electromagnetic size:

$$r_{[ud]_{0^+}} \gtrsim r_\pi, \qquad r_{\{uu\}_{1^+}} \gtrsim r_\rho, \qquad r_{\{uu\}_{1^+}} > r_{[ud]_{0^+}}$$

Diquark species

Octet and decuplet baryons

	[nn]	{nn}	[ns]	{ns}	{ss}
N	●	●			
Δ		●			
Λ	●		●	●	
Σ		●	●	●	
Ξ			●	●	●
Ω					●

Other baryons as parity partners

- ☞ $[I=0, J^P=0^+]$: Isoscalar-scalar.
- ☞ $[I=1, J^P=1^+]$: Isovector-pseudovector.
- ☞ $[I=0, J^P=0^-]$: Isoscalar-pseudoscalar.
- ☞ $[I=0, J^P=1^-]$: Isoscalar-vector.
- ☞ $[I=1, J^P=1^-]$: Isovector-vector.

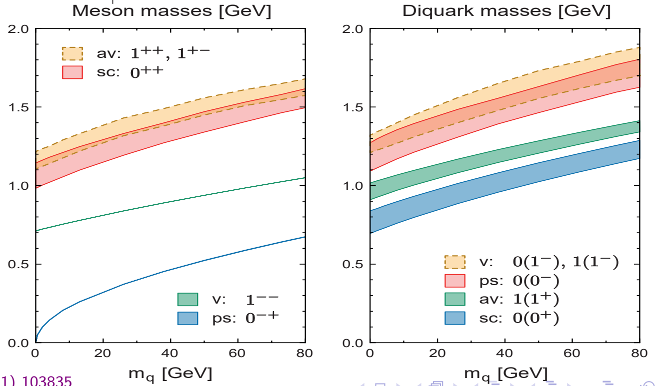

M. Yu. Barabanov *et al.*,
Prog. Part. Nucl. Phys. 116 (2021) 103835

The quark+diquark structure of a baryon

☞ A baryon can be viewed as a **Borromean bound-state**, the binding within which has two contributions:

- Formation of tight diquark correlations.
- Quark exchange depicted in the shaded area.

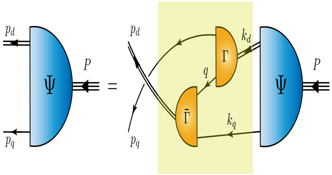

☞ The exchange ensures that diquark correlations within the baryon are fully dynamical: no quark holds a special place.

☞ The rearrangement of the quarks guarantees that the baryon's wave function complies with Pauli statistics.

☞ The number of states in the spectrum of baryons obtained is similar to that found in the three-constituent quark model, just as it is in today's LQCD calculations.

☞ Modern diquarks are different from the old static, point-like diquarks which featured in early attempts to explain the so-called missing resonance problem.

☞ Modern diquarks enforce certain distinct interaction patterns for the singly- and doubly-represented valence-quarks within the baryon.

S.-S. Xu *et al.*, Phys. Rev. D92 (2015) 114034; Y. Lu *et al.*, Phys. Rev. C96 (2017) 015208;
C. Chen *et al.*, Phys. Rev. D100 (2019) 054009; P.-L. Yin *et al.*, Phys. Rev. D100 (2019) 034008.

- The computed masses are uniformly larger than the corresponding empirical values.
- The quark-diquark kernel omits all resonant contributions associated with meson-baryon final state interactions, which typically generate a measurable reduction.
- The Faddeev equations analyzed to produce the results should be understood as producing the dressed-quark core of the bound state, not the completely dressed and hence observable object.

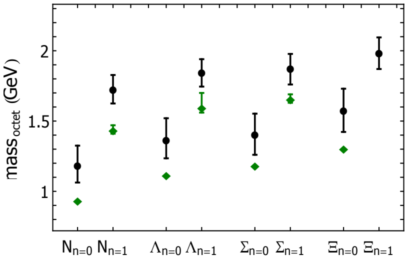

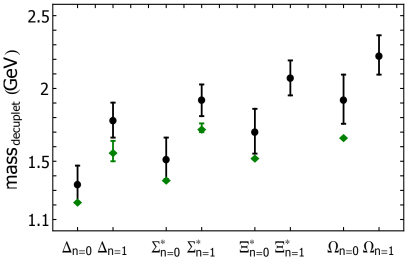

C. Chen *et al.*, Phys. Rev. D100 (2019) 054009.

Diquark content of the octet and decuplet

Only axial-vector diquarks are present in the decuplet baryons. For the octet case...

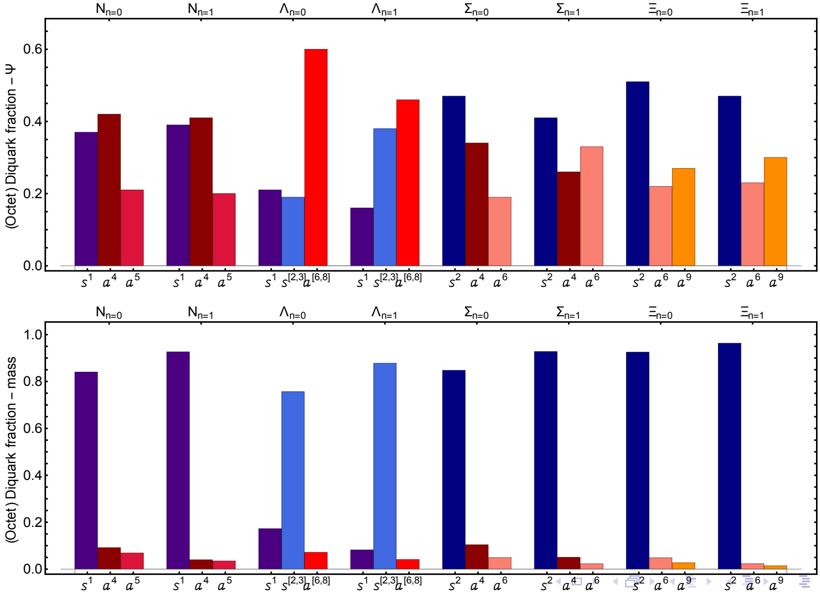

A measurable consequence of diquark content

$\Lambda - \Sigma$ mass splitting

Whilst the Λ and Σ are associated with the same combination of valence-quarks, their spin-flavor wave functions are different.

$$\Downarrow$$

Λ contains more of the (lighter) scalar diquark correlations than Σ

$$u_\Lambda = \frac{1}{\sqrt{2}} \begin{bmatrix} \sqrt{2}\, s[ud]_{0^+} \\ d[us]_{0^+} - u[ds]_{0^+} \\ d\{us\}_{1^+} - u\{ds\}_{1^+} \end{bmatrix} \leftrightarrow \begin{bmatrix} s_\Lambda^1 \\ s_\Lambda^{[2,3]} \\ a_\Lambda^{[6,8]} \end{bmatrix} \; ; \quad u_\Sigma = \begin{bmatrix} u[us]_{0^+} \\ s\{uu\}_{1^+} \\ u\{us\}_{1^+} \end{bmatrix} \leftrightarrow \begin{bmatrix} s_\Sigma^2 \\ a_\Sigma^4 \\ a_\Sigma^6 \end{bmatrix}$$

	N	Λ	Σ	Ξ	Δ	Σ^*	Ξ^*	Ω
The.	1.19(13)	1.37(14)	1.41(14)	1.58(15)	1.35(12)	1.52(14)	1.71(15)	1.93(17)
Exp.	0.94	1.12	1.19	1.31	1.23	1.38	1.53	1.67
The.	1.73(10)	1.85(09)	1.88(11)	1.99(11)	1.79(12)	1.93(11)	2.08(12)	2.23(13)
Exp.	1.44(03)	$1.51^{+0.10}_{-0.04}$	1.66(03)	-	1.57(07)	1.73(03)	-	-

non-relativistic | **relativistic**

Mesons: $P = (-1)^{L+1}$

S	L	J^{PC}
0	0	0^{-+}
1	0	1^{--}
0	1	1^{+-}
1	1	0^{++}

~~$P = (-1)^{L+1}$~~

Bethe,Salpeter, Llewelyn-Smith 1950ies

$$\Gamma_\pi(P,p) = \gamma_5 \left[F_1(P,p) + F_2(P,p) i\not{P} + F_3(P,p) pP i\not{p} + F_4(P,p)[\not{p}, \not{P}]\right]$$

s-wave: F_1, F_2; p-wave: F_3, F_4

Baryons: $P = (-1)^{L}$

S	L	J^P
1/2	0	$1/2^+$
3/2	2	

~~$P = (-1)^{L}$~~

J^P	total	s-wave	p-wave	d-wave	f-wave
$1/2^+$	64	8	36	20	
$3/2^+$	128	4	36	60	28

The P- and D-wave components play a measurable role in octet and decuplet baryons

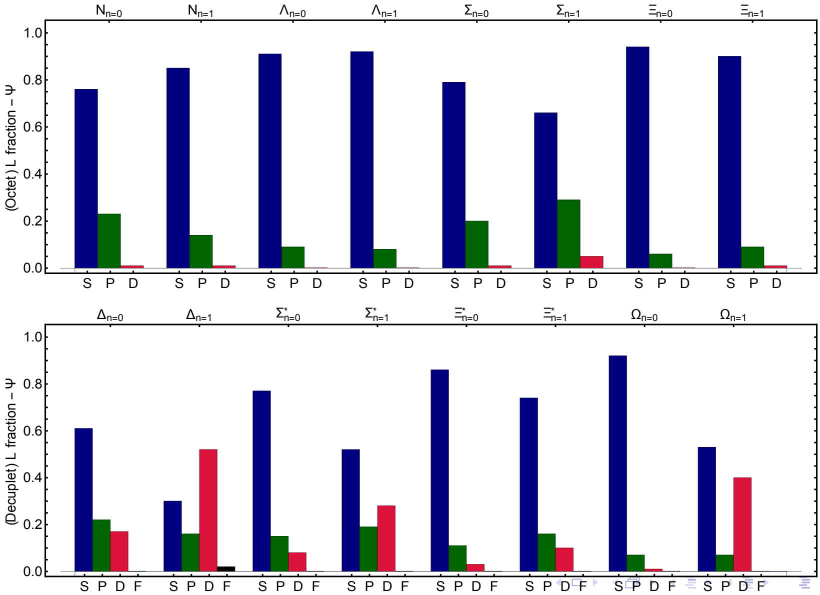

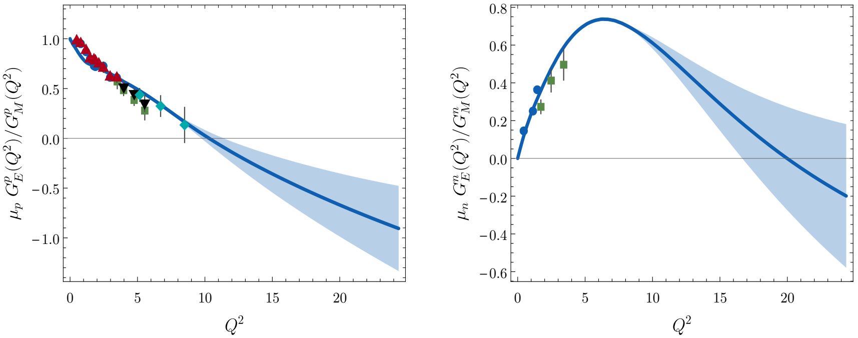

Z.-F. Cui *et al.*, Phys. Rev. D102 (2020) 014043.

☞ Observations:

- There is no evidence for scaling in Dirac and Pauli form factors, and thus in the electromagnetic Sach form factors.
- Our analysis predicts a zero for the proton's electromagnetic ratio at $Q^2 = 10.3^{+1.1}_{-0.7}\,\text{GeV}^2$.
- The neutron's electromagnetic ratio has a peak at $Q^2 \approx 6\,\text{GeV}^2$ and then crosses zero for $Q^2 = 20.1^{+10.6}_{-3.5}\,\text{GeV}^2$.
- All these features can be related with both quark-quark and angular momentum correlations within the nucleon.

The $\gamma^{(*)} N(940) \to N(940)$ reaction (II)

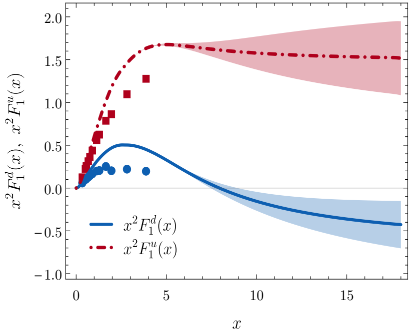

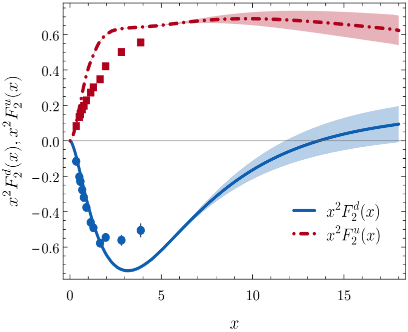

☞ Observations:

- F_1^d is smaller than F_1^u, even allowing for the difference in normalisation, and decreases more quickly as $x = Q^2/m_N^2$ increases.
- The location of the zero in F_1^d is a measure of the relative probability of finding pseudovector and scalar diquarks in the proton.
- The u- and d-quark Pauli form factors are roughly equal in magnitude on $x \lesssim 5$; *i.e.* F_2^d is suppressed with respect F_2^u but only at large momentum transfer.
- There are contributions playing an important role in F_2, like the anomalous magnetic moment of dressed-quarks or meson-baryon final-state interactions.

PRL **104,** 042302 (2010) PHYSICAL REVIEW LETTERS week ending 29 JANUARY 2010

Disentangling the Dynamical Origin of P_{11} Nucleon Resonances

N. Suzuki,[1,2] B. Juliá-Díaz,[3,2] H. Kamano,[2] T.-S. H. Lee,[2,4] A. Matsuyama,[5,2] and T. Sato[1,2]

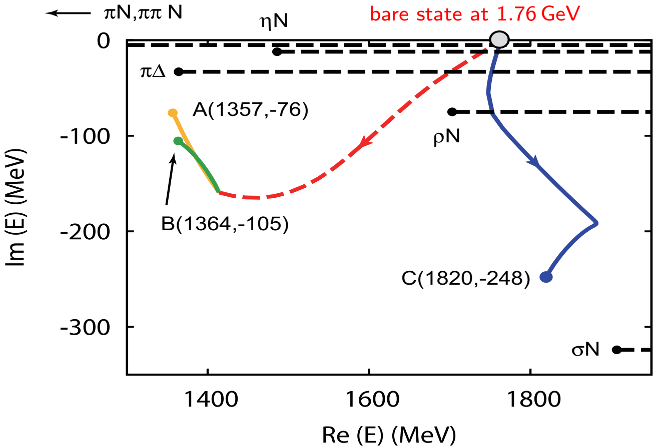

The Roper is the proton's first radial excitation. *Its unexpectedly low mass arise from a dressed-quark core that is shielded by a meson-cloud which acts to diminish its mass.*

Bound-state kernels which omit meson-cloud corrections produce masses for hadrons that are larger than the empirical values (in GeV):

$$M_{Roper}^{DSE} = 1.73 \, GeV \qquad M_{Roper}^{EBAC} = 1.76 \, GeV$$

☞ Observation:

- Meson-Baryon final state interactions reduce dressed-quark core mass by $(10 - 20)\%$. The cloud's impact depends on the state's quantum numbers.
- Roper and Nucleon have very similar wave functions and diquark content.
- A single zero in S-wave components of the wave function $\Rightarrow$ A radial excitation.

0th Chebyshev moment of the S-wave components

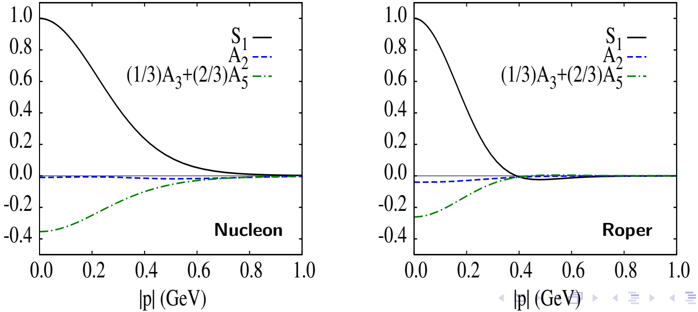

Nucleon-to-Roper transition form factors at high virtual photon momenta penetrate the meson-cloud and thereby illuminate the dressed-quark core

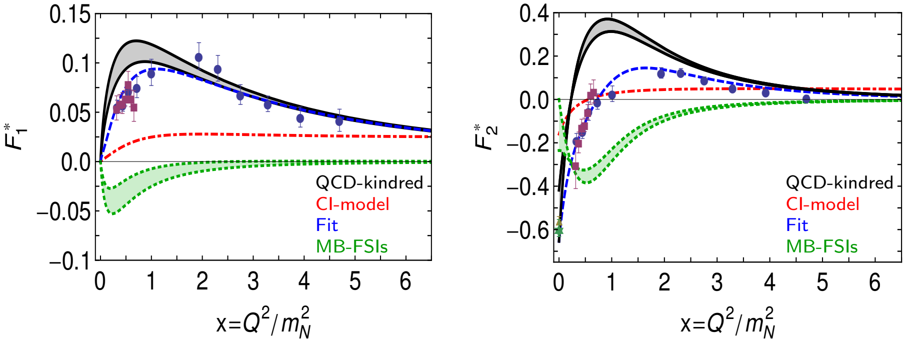

☞ Observations:

- Our calculation agrees quantitatively in magnitude and qualitatively in trend with the data on $x \gtrsim 2$.
- The mismatch between our prediction and the data on $x \lesssim 2$ is due to meson cloud contribution.
- The dotted-green curve is an inferred form of meson cloud contribution from the fit to the data.

CLAS12 at JLab aims to deliver data on the Roper-resonance electroproduction form factors out to $Q^2 \sim 12 m_N^2$ in both charged and neutral channels

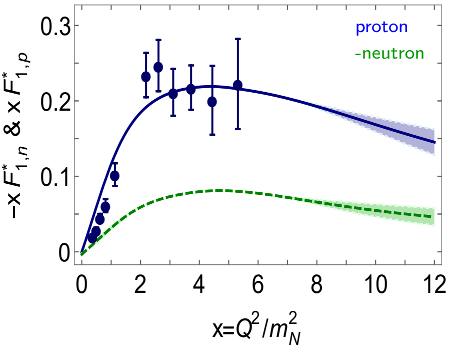

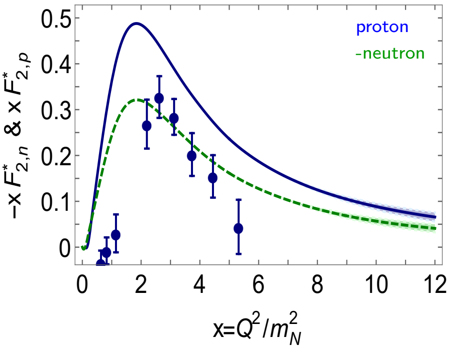

☞ Observations:

- On the domain depicted, there is no indication of the scaling behavior expected of the transition form factors: $F_1^* \sim 1/x^2$, $F_2^* \sim 1/x^3$.
- Since each dressed-quark in the baryons must roughly share the momentum, Q, we expect that such behaviour will only become evident on $x \gtrsim 20$.

Barycentric plots: *left panel* – conformal limit PDA, $\varphi_N^{\rm cl}([x]) = 120 x_1 x_2 x_3$; *middle panel* – computed proton PDA evolved to $\zeta = 2$ GeV, which peaks at $([x]) = (0.55, 0.23, 0.22)$; and *right panel* – Roper resonance PDA at $\zeta = 2$ GeV. The white circle in each panel serves only to mark the centre of mass for the conformal PDA, whose peak lies at $([x]) = (1/3, 1/3, 1/3)$.

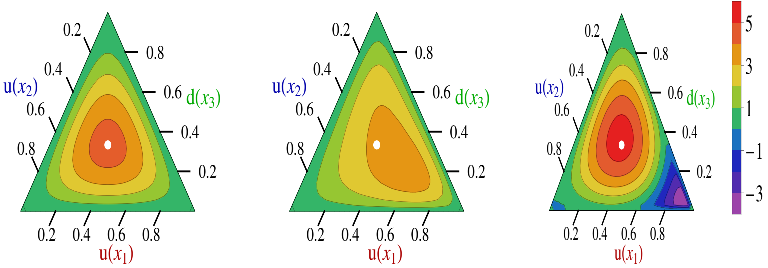

☞ Observations:

- Proton: The leading-twist PDA of the ground-state nucleon is both broader than $\varphi_N^{\rm cl}([x])$ and decreases monotonically away from its maximum in all directions.
- Proton: The peak of the φ-distribution is shifted toward the region where the single quark carries most of the nucleon light-cone momentum fraction.
- Roper: The excitation's PDA is not positive definite which echos features of the wave function for the first radial excitation of a quantum mechanical system.

C. Mezrag *et al.*, Phys. Lett. B783 (2018) 263.

Nucleon and Roper PDAs (II)

C. Mezrag *et al.*, Phys. Lett. B783 (2018) 263.

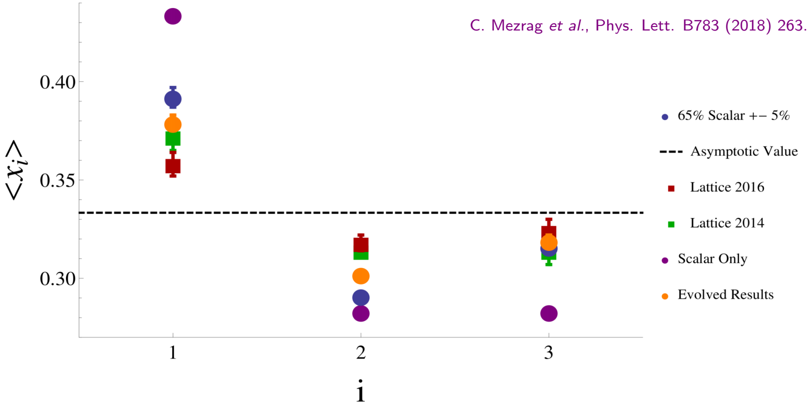

	Scalar	S+AV	Evolved	Braun:2014wpa	Bali:2015ykx
$\langle x_1 \rangle_\varphi$	0.434	0.392(5)	0.379(4)	0.372(7)	0.358(6)
$\langle x_2 \rangle_\varphi$	0.283	0.291(2)	0.302(1)	0.314(3)	0.319(4)
$\langle x_3 \rangle_\varphi$	0.283	0.316(4)	0.319(3)	0.314(7)	0.323(6)
$10^3\, f_N$ (GeV^2)	2.97	4.05	3.78(14)	2.84(33)	3.60(6)

$G^*_{M,J\text{-}S}$ *cf. Experimental data and EBAC analysis*

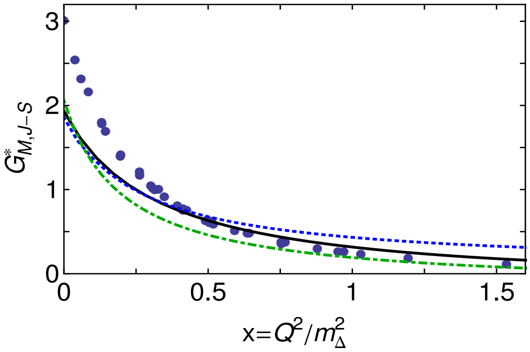

- Solid-black: QCD-kindred interaction.
- Dashed-blue: Contact interaction.
- Dot-Dashed-green: Dynamical + no meson-cloud

☞ Observations:

- All curves are in marked disagreement at infrared momenta.
- Similarity between Solid-black and Dot-Dashed-green.
- The discrepancy at infrared comes from omission of meson-cloud effects.
- Both curves are consistent with data for $Q^2 \gtrsim 0.75 m^2_\Delta \sim 1.14\,\text{GeV}^2$.

☞ $R_{EM} = R_{SM} = 0$ in SU(6)-symmetric CQM.

- Deformation of the hadrons involved.
- Modification of the transition current.

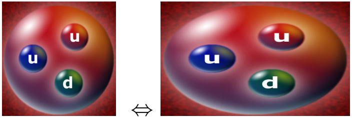

☞ R_{SM}: Good description of the rapid fall at large momentum transfer.

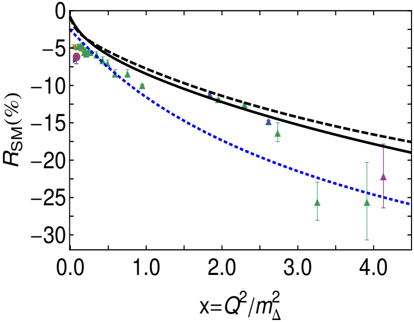

☞ R_{EM}: A particularly sensitive measure of orbital angular momentum correlations.

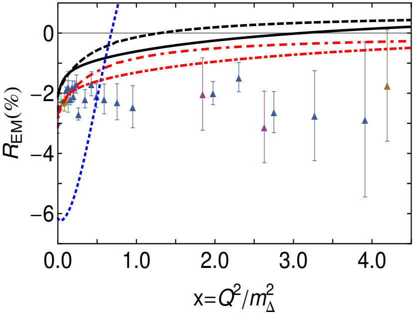

☞ *Zero Crossing in the electric transition form factor:*

$$\text{Contact interaction} \to Q^2 \sim 0.75 m_\Delta^2 \sim 1.14\ GeV^2$$

$$\text{QCD-kindred interaction} \to Q^2 \sim 3.25 m_\Delta^2 \sim 4.93\ GeV^2$$

Helicity conservation arguments in pQCD should apply equally to:

- *Results obtained within our QCD-kindred framework;*
- *Results produced by a symmetry-preserving treatment of a contact interaction.*

$$R_{EM} \overset{Q^2 \to \infty}{=} 1\,, \quad R_{SM} \overset{Q^2 \to \infty}{=} constant\,.$$

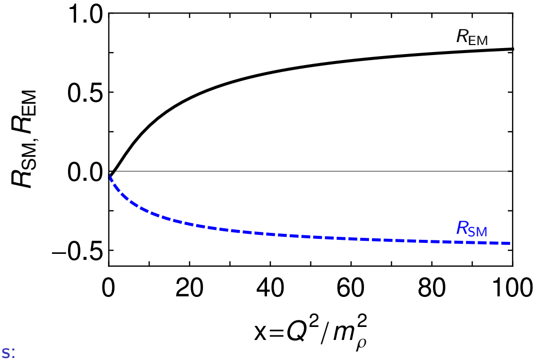

☞ Observations:

- Truly asymptotic Q^2 is required before predictions are realized.
- $R_{EM} = 0$ at an empirical accessible momentum and then $R_{EM} \to 1$.
- $R_{SM} \to$ constant. Curve contains the logarithmic corrections expected in QCD.

	$N(940)$	$N(1440)$	$\Delta(1232)$	$\Delta(1600)$
S-wave	0.76	0.85	0.61	0.30
P-wave	0.23	0.14	0.22	0.15
D-wave	0.01	0.01	0.17	0.52
F-wave	—	—	~ 0	0.02

$N(1440)$

- Roper's diquark content are almost identical to the nucleon's one.
- It has an orbital angular momentum composition which is very similar to the one observed in the nucleon.

$\Delta(1600)$

- $\Delta(1600)$'s diquark content are almost identical to the $\Delta(1232)$'s one.
- It shows a dominant $\ell = 2$ angular momentum component with its S-wave term being a factor 2 smaller.

0th Chebyshev moment of the S-wave component

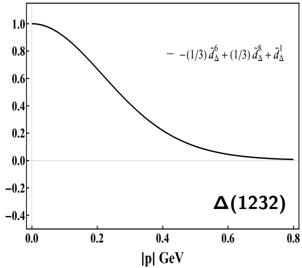

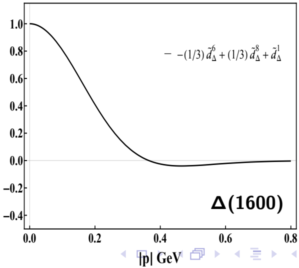

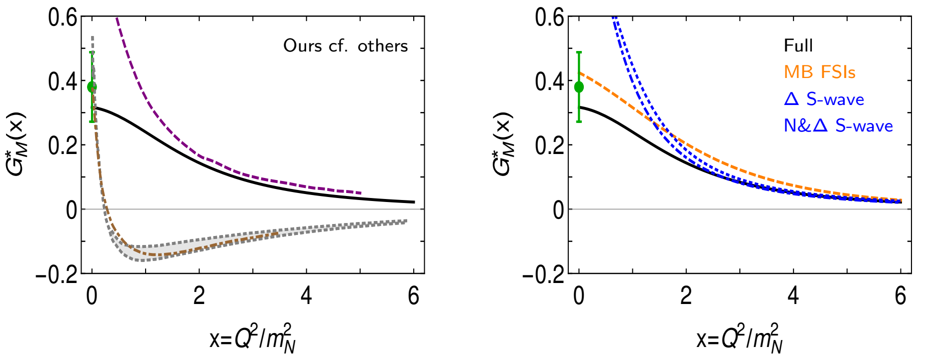

☞ Observations:

- It is positive defined in the whole range of photon momentum and decreases smoothly with larger Q^2-values.
- The mismatch with the empirical result are comparable with that in the $\Delta(1232)$ case, suggesting that MB FSIs are of similar importance in both channels.
- Higher partial-waves have a visible impact on G_M^*: They bring the magnetic dipole moment to lower values which could be compatible with experiment.

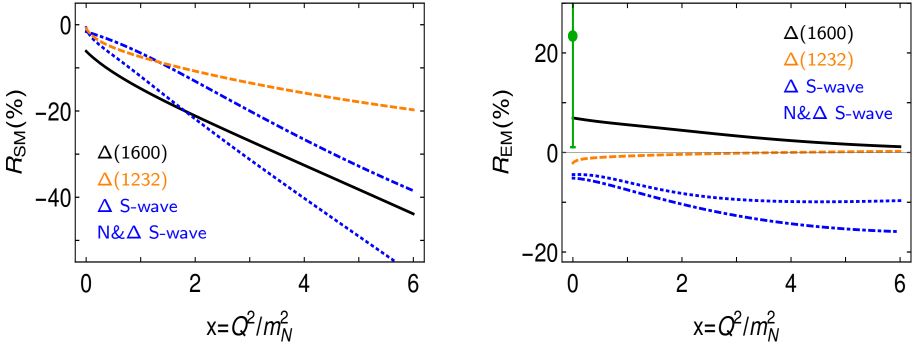

☞ Observations:

- $R_{SM}^{\Delta'} \gtrsim R_{SM}^{\Delta}$ indicating that higher orbital angular momentum components in the Δ(1600) are more important than in the Δ(1232).
- R_{EM} for the Δ(1600) transition is far larger in magnitude than the analogous result for the Δ(1232) (and opposite in sign).
- Points above are an observable manifestation of important higher orbital angular momentum components in both states.
- In particular, there is an enhanced *D*-wave strength in the Δ(1600) relative to that in the Δ(1232).

Epilogue

☞ The wealth of new and anticipated information demands that the issue of correlations within hadrons be settled.

- The features of baryons, and their unification with the properties of mesons, depend on a veracious expression of EHM in the hadron's bound-state and scattering problems.
- The existence of non-pointlike, fully dynamical quark-quark correlations is an important consequence of EHM. There is evidence for such clusters in simulations of lQCD..
- Poincaré covariance demands the presence of dressed-quark orbital angular momentum in the baryon, and it is predicted to have numerous observable consequences.

☞ Modern facilities will probe hadronic interiors as never before.

- JLab-12 and -22 will push form factor measurements to unprecedented values of momentum transfer and use different charge states, enabling flavour separations.
- COMPASS, EIC and EicC would measure valence-quark distribution functions with previously unattainable precision.
- Collaborations like Belle-II, BES-III and LHCb, are discovering new hadrons whose structure does not fit once viable paradigms.

M. Yu. Barabanov *et al.*,
Prog. Part. Nucl. Phys. 116 (2021) 103835